

Effects of the scalar mesons in a Skyrme model with hidden local symmetry

Bing-Ran He,^{1,*} Yong-Liang Ma,^{2,†} and Masayasu Harada^{1,‡}

¹*Department of Physics, Nagoya University, Nagoya, 464-8602, Japan*

²*Center of Theoretical Physics and College of Physics, Jilin University, Changchun, 130012, China*

(Dated: December 23, 2018)

We study the effects of light scalar mesons on the skyrmion properties by first constructing a mesonic model including pion, rho and omega mesons as well as a two-quark and a four-quark scalar states. In our model, the physical scalar mesons are defined as mixing states of the two- and four-quark states. We find that the scalar mesons reduce the skyrmion mass as expected and the lighter scalar meson is, the smaller soliton mass and larger soliton size become when there are no direct coupling between the scalar mesons and the vector mesons. When the direct coupling becomes stronger, the soliton becomes heavier and the charge radius of the baryon number density becomes larger since the repulsive force arising from the ω meson becomes stronger. For the effect of the mixing, we find that, when the magnitude of the two-quark component of the lighter scalar meson is increased, the soliton mass becomes smaller and the soliton size becomes larger.

PACS numbers: 11.30.Rd, 12.39.Dc, 12.39.Fe, 14.40.Be

I. INTRODUCTION

More than fifty years ago, T. H. R. Skyrme proposed his pioneer idea that one may identify a certain non-trivial topological field configuration (soliton) in a mesonic theory with baryon [1]. Since then, this idea was extensively applied in particle physics, nuclear physics and also condensate matter physics [2]. In the originally proposed Skyrme model, only the degree of freedom of pion is included. Motivated by the essential roles of resonances, such as the rho meson, omega meson, and light scalar mesons in nuclear physics, for example to obtain the empirical nuclear force, people extended the Skyrme model to Skyrme-type models including such resonances [3, 4].

Recently, especially after the arising of the holographic models of QCD, effects of some resonances were widely explored. Some key points related to the present work are summarized as follows: (i) By dimensionally deconstructing a Yang-Mills theory in the flat four-dimensional space in the large N_c limit, it was found that the more iso-vector vector resonances included, the lighter soliton is [5]. (ii) By using a chiral effective theories of vector mesons based on the hidden local symmetry (HLS) approach written including the terms at the next to leading order, people found that the omega meson which enters into the chiral effective theory through the homogeneous Wess-Zumino term provides a strong repulsive force [6, 7]. (iii) A scalar meson was introduced to the HLS Lagrangian, by regarding it as the Nambu-Golstone boson associated with the spontaneous breaking of scale symmetry, i.e., dilaton, to investigate the attractive effect from it [8–10]. It was found that, the dilaton can provide

about 100 MeV attractive force in the model which can reproduce the chiral restoration in matter.

In this paper, we explore the effect of the scalar mesons made of two quarks and four quarks on the mass and the size of the skyrmion by first constructing a chiral effective model including pion, rho, omega and two scalar mesons. Then, determining the parameters in the model through the meson dynamics, we study the effects of the masses and constituents of the scalar mesons as well as the strength of an interaction among the vector and scalar mesons on the mass and radii of the skyrmion.

What we have found in this work can be summarized as follows:

1. When we switch off the mixing between the two-quark and four-quark states in the model, the four-quark scalar is decoupled from the model. In such a case, we find that the soliton mass decreases with the increase of the mass of the light scalar meson, here, a pure two-quark state. In addition, we find that the soliton size decreases with the increase of the light scalar meson mass.
2. We study the soliton mass as a function of the coupling strength between the scalar meson and vector meson. Our result shows that soliton mass decreases when the coupling becomes stronger.
3. When the mixing between the two-quark and four-quark states is included in the model, we find that, when the two-quark component in the lighter scalar meson is larger, the soliton mass is lighter and the size is larger.

This paper is organized as follows: In sec. II we construct a chiral effective model which we use in this paper and explain its typical characters related to this work. We make a numerical calculation of the skyrmion properties and analyse the effects of scalar mesons on them in sec. III. Our conclusions and discussions are given in the

* he@hken.phys.nagoya-u.ac.jp

† yongliangma@jlu.edu.cn

‡ harada@hken.phys.nagoya-u.ac.jp

last section. Some details of the calculation are given in the appendix.

II. THE MODEL

We start from the construction of a chiral effective model including a two-quark and a four-quark scalar mesons. Here, we limit our discussion to mesons including up and down quarks. In our model, we introduce a two-quark field $M_{(2)}$ which schematically written in the quark level as

$$(M_{(2)})_i^j \sim \bar{q}_{Ri} q_{Lj} , \quad (1)$$

with $i, j = 1, 2$. This, in the hadron level, is constructed from the iso-singlet σ field and the iso-triplet π fields as

$$M_{(2)} = \frac{1}{2} (\sigma + i\vec{\pi} \cdot \vec{\tau}) , \quad (2)$$

where $\vec{\tau}$ are the Pauli matrices. Under chiral transformation, the matrix $M_{(2)}$ transforms as

$$M_{(2)} \rightarrow g_L M_{(2)} g_R^\dagger , \quad (3)$$

where $g_{L,R} \in \text{SU}(2)_{L,R}$. Furthermore, from the quark level, we can impose the Z_2 symmetry as a remnant of the $\text{U}(1)_A$ transformation under which q_L and q_R transform as $q_L \rightarrow -q_L$ and $q_R \rightarrow q_R$. Then, the hadron field $M_{(2)}$ transforms as

$$M_{(2)} \rightarrow -M_{(2)} , \quad (4)$$

We introduce a four-quark state which is schematically written in the quark level as

$$\phi \sim \bar{q}_{Li} \bar{q}_{Lj} \epsilon^{ij} q_R^k q_R^l \epsilon_{kl} . \quad (5)$$

In the present work, we regard ϕ as a real field by considering the real part of Eq. (5). Under the Z_2 transformation, ϕ transforms as

$$\phi \rightarrow \phi . \quad (6)$$

Based on the chiral symmetry together with the Z_2 symmetry and an assumption of the non-derivative type interactions, the Lagrangian is written in the form

$$\begin{aligned} \mathcal{L} = & \text{Tr} \left(\partial_\mu M_{(2)} \partial^\mu M_{(2)}^\dagger \right) + \frac{1}{2} \partial_\mu \phi \partial^\mu \phi \\ & - (V_0 - \bar{V}_0) - (V_{\text{SB}} - \bar{V}_{\text{SB}}) , \end{aligned} \quad (7)$$

where V_0 stands for the meson potential term and V_{SB} denotes the explicit chiral symmetry breaking term with \bar{V}_0 and \bar{V}_{SB} as their corresponding values in vacuum.

We require that the number of fields in each vertex derived from the potential V_0 are less than or equal to four legs. Furthermore, as in Ref. [11], by requiring that the number of quarks included in each vertex are less than or equal to eight, the potential is expressed as

$$\begin{aligned} V_0 = & \lambda \text{Tr} \left(M_{(2)} M_{(2)}^\dagger M_{(2)} M_{(2)}^\dagger \right) - m_2^2 \text{Tr} \left(M_{(2)} M_{(2)}^\dagger \right) + \frac{1}{2} m_4^2 \phi^2 \\ & + \sqrt{2} A \left(\det \left(M_{(2)} \right) + \det \left(M_{(2)}^\dagger \right) \right) \phi . \end{aligned} \quad (8)$$

As for the explicit chiral symmetry breaking potential V_{SB} , we adopt the simplest form:

$$V_{\text{SB}} = -\frac{1}{2} f_\pi \text{Tr} \left(\chi M_{(2)}^\dagger + \chi^\dagger M_{(2)} \right) , \quad (9)$$

where $\chi = 2B\mathcal{M}$ with B and \mathcal{M} being a constant with dimension one and the quark mass matrix. In the present analysis, we neglect the effect of isospin breaking due to the current quark mass: $\mathcal{M} = \text{diag}(\bar{m}, \bar{m})$ with $\bar{m} = (m_u + m_d)/2$. We use the pion mass as an input to determine the relevant parameters, so that V_{SB} in the present form is expressed as

$$V_{\text{SB}} = -\frac{1}{2} f_\pi m_\pi^2 \text{Tr} \left(M_{(2)}^\dagger + M_{(2)} \right) . \quad (10)$$

In this paper, we introduce the rho and omega mesons based on the hidden local symmetry (HLS) [12, 13]. For

this purpose, we take the polar decomposition of $M_{(2)}$ as $M_{(2)} = \frac{1}{2} \xi_L^\dagger \sigma \xi_R$ where ξ_L and ξ_R in the unitary gauge of the HLS are expressed by the pion fields as

$$\xi_R = \xi_L^\dagger = e^{i\vec{\pi} \cdot \vec{\tau} / (2f_\pi)} . \quad (11)$$

Then, we write the Lagrangian (7) as

$$\begin{aligned} \mathcal{L} = & \frac{1}{2} \partial_\mu \sigma \partial^\mu \sigma + \sigma^2 \text{Tr} \left(\alpha_{\perp\mu} \alpha_{\perp}^\mu \right) + \frac{1}{2} \partial_\mu \phi \partial^\mu \phi \\ & - (V_0 - \bar{V}_0) - (V_{\text{SB}} - \bar{V}_{\text{SB}}) + \mathcal{L}_V , \end{aligned} \quad (12)$$

where

$$\alpha_{\perp\mu} = \frac{1}{2i} \left(\partial_\mu \xi_R \cdot \xi_R^\dagger - \partial_\mu \xi_L \cdot \xi_L^\dagger \right) , \quad (13)$$

and \mathcal{L}_V represents the Lagrangian for the rho and omega mesons, which we will give an explicit form later. The

potential V_0 and V_{SB} are rewritten as

$$\begin{aligned} V_0 &= \frac{1}{8}\lambda\sigma^4 - \frac{1}{2}m_2^2\sigma^2 + \frac{1}{2}m_4^2\phi^2 + \frac{1}{\sqrt{2}}A\sigma^2\phi, \\ V_{\text{SB}} &= -\frac{1}{4}m_\pi^2 f_\pi \sigma \text{Tr}(U + U^\dagger), \end{aligned} \quad (14)$$

with $U = \xi_L^\dagger \xi_R = e^{i\vec{\pi}\vec{\tau}/f_\pi}$.

The minima of the potential of the system are obtained by taking the first order derivative of the potential $V = V_0 + V_{\text{SB}}$ with respect to σ and ϕ . The expressions are

$$\frac{\partial V}{\partial \sigma} = \frac{1}{2}\lambda\sigma^3 - m_2^2\sigma + \sqrt{2}A\sigma\phi - m_\pi^2 f_\pi, \quad (15)$$

$$\frac{\partial V}{\partial \phi} = m_4^2\phi + \frac{1}{\sqrt{2}}A\sigma^2. \quad (16)$$

After a suitable choice of the parameters in the model, σ acquires its expectation value σ_{vac} and therefore, for a non-zero A , ϕ also has its expectation value ϕ_{vac} . The physical scalar meson fields are obtained from the fluctuations with respect to the relevant expectation values through $\sigma = \sigma_{\text{vac}} + \tilde{\sigma} \equiv f_\pi + \tilde{\sigma}$, $\phi = \phi_{\text{vac}} + \tilde{\phi}$ with f_π being the pion decay constant and $\phi_{\text{vac}} = -\frac{Af_\pi^2}{\sqrt{2}m_4^2}$ given in Eq. (A4).

Taking the second order derivative, one can get the mass matrix of σ and ϕ as

$$\begin{pmatrix} m_\sigma^2 & m_{\sigma\phi}^2 \\ m_{\phi\sigma}^2 & m_\phi^2 \end{pmatrix} = \begin{pmatrix} \lambda f_\pi^2 + m_\pi^2 & \sqrt{2}A f_\pi \\ \sqrt{2}A f_\pi & m_4^2 \end{pmatrix}. \quad (17)$$

The physical states denoted as f_{500} and f_{1370} are related to σ and ϕ as

$$\begin{pmatrix} f_{500} \\ f_{1370} \end{pmatrix} = \begin{pmatrix} \cos\theta & -\sin\theta \\ \sin\theta & \cos\theta \end{pmatrix} \begin{pmatrix} \tilde{\sigma} \\ \tilde{\phi} \end{pmatrix}, \quad (18)$$

where θ is the mixing angle. In Appendix A, we show some relations among the parameters and the physical quantities which may be useful. From Eq. (18) one can see that when $\cos\theta \rightarrow 0$, the physical state f_{500} is dominantly a four-quark state and f_{1370} is the two-quark state. On the other hand, when $\cos\theta \rightarrow 1$, f_{500} is almost a two-quark state but f_{1370} is almost a four-quark state.

Now, we are in the position to specify the vector meson part of the Lagrangian. Here we take the following form:

$$\mathcal{L}_V = \mathcal{L}_{V_0} + \mathcal{L}_{\text{anom}}, \quad (19)$$

where \mathcal{L}_{V_0} is the Lagrangian with only intrinsic parity even terms, while $\mathcal{L}_{\text{anom}}$ contains the intrinsic parity violating terms related to the $\text{SU}(2)_L \times \text{SU}(2)_R \times \text{U}(1)_V$ anomaly.

More explicitly, the intrinsic parity even Lagrangian \mathcal{L}_{V_0} is expressed as

$$\begin{aligned} \mathcal{L}_{V_0} &= a_{\text{hls}}(s_0\sigma^2 + (1-s_0)F^2) \text{Tr}(\hat{\alpha}_{\parallel\mu}\hat{\alpha}_{\parallel\mu}^\dagger) \\ &\quad - \frac{1}{2g^2} \text{Tr}(V_{\mu\nu}V^{\mu\nu}). \end{aligned} \quad (20)$$

where $\hat{\alpha}_{\parallel\mu}^\dagger$ and $V_{\mu\nu}$ are defined as

$$\begin{aligned} \hat{\alpha}_{\parallel\mu} &= \frac{1}{2i} \left(\partial_\mu \xi_R \cdot \xi_R^\dagger + \partial_\mu \xi_L \cdot \xi_L^\dagger \right) - V_\mu, \\ V_{\mu\nu} &\equiv \partial_\mu V_\nu - \partial_\nu V_\mu - i[V_\mu, V_\nu], \end{aligned} \quad (21)$$

with

$$V_\mu = \frac{g}{\sqrt{2}} \begin{pmatrix} \frac{1}{\sqrt{2}}(\rho_\mu^0 + \omega_\mu) & \\ & \rho_\mu^- \\ & & \rho_\mu^+ \\ & & & -\frac{1}{\sqrt{2}}(\rho_\mu^0 + \omega_\mu) \end{pmatrix}. \quad (22)$$

Here g is the gauge coupling constant of the HLS, a_{hls} and s_0 are the real dimensionless parameters and F is a constant with the dimension one. When the σ has its VEV as $\sigma_{\text{vac}} = f_\pi$, the vector meson mass is expressed as $m_V^2 = a_{\text{hls}}g^2(s_0f_\pi^2 + (1-s_0)F^2)$, in which $a_{\text{hls}}g^2s_0f_\pi^2$ stands for the mass obtained by the spontaneous chiral symmetry breaking and $a_{\text{hls}}g^2(1-s_0)F^2$ is the chiral invariant mass. In this paper, we take $F = f_\pi$ in such a way that s_0 is the percentage of the vector meson mass coming from the spontaneous chiral symmetry breaking. We should notice that the existence of the Z_2 symmetry leads to the absence of the term linear in σ field, and that s_0 could be both positive and negative.

The anomaly term of Lagrangian $\mathcal{L}_{\text{anom}}$ in Eq. (19) reads [13]

$$\int d^4x \mathcal{L}_{\text{anom}} = \frac{N_c}{16\pi^2} \int_{M^4} \sum_{i=1}^3 c_i \mathcal{L}_i, \quad (23)$$

where M^4 stands for the four-dimensional Minkowski space and

$$\mathcal{L}_1 = i\epsilon^{\mu\nu\sigma\rho} \text{Tr}(\alpha_{L\mu}\alpha_{L\nu}\alpha_{L\sigma}\alpha_{R\rho} - \alpha_{R\mu}\alpha_{R\nu}\alpha_{R\sigma}\alpha_{L\rho}), \quad (24)$$

$$\mathcal{L}_2 = i\epsilon^{\mu\nu\sigma\rho} \text{Tr}(\alpha_{L\mu}\alpha_{R\nu}\alpha_{L\sigma}\alpha_{R\rho}), \quad (25)$$

$$\mathcal{L}_3 = \epsilon^{\mu\nu\sigma\rho} \text{Tr}[F_{V\mu\nu}(\alpha_{L\sigma}\alpha_{R\rho} - \alpha_{R\sigma}\alpha_{L\rho})], \quad (26)$$

in terms of the 1-form and 2-form notations with $\alpha_L = \hat{\alpha}_{\parallel} - \alpha_{\perp}$, $\alpha_R = \hat{\alpha}_{\parallel} + \alpha_{\perp}$, $F_V = dV - iV^2$. Since it is difficult to fix the the low energy constants c_1, c_2 and c_3 from the fundamental QCD, the values are usually estimated from phenomenologically with respect to the experimental data [13]. But here, for a simple study of the scalar meson effects on the skyrmion properties, we select $c_1 = -c_2 = -2/3$ and $c_3 = 0$ which agrees with the minimal model [14] in which the omega meson coupling to the baryon number current $\omega_\mu B^\mu$ is included.

III. NUMERICAL RESULTS FOR THE SKYRMION

In this section we make a numerical study of the effects of scalar mesons on the mass and charge radii of the baryon number and the soliton energy. In Table. I, we summarize the parameters of the model used in this paper.

f_π	92.4 MeV
m_π	139.57 MeV
N_c	3
$c_1 + c_2$	0
$c_1 - c_2$	-4/3
c_3	0
g	5.80 ± 0.91
a_{hls}	2.07 ± 0.33

TABLE I: Values of the model parameters.

A. The ansatz

In order to study the properties of the soliton obtained from the Lagrangian (12), we take the standard parameterization for the soliton configurations. Following Refs. [1, 14], we take the ansatz for π , ρ and ω fields as

$$U = e^{i\boldsymbol{\tau} \cdot \hat{\mathbf{r}} F(r)}, \quad (27a)$$

$$\boldsymbol{\rho} = \frac{G(r)}{gr} (\hat{\mathbf{r}} \times \boldsymbol{\tau}), \quad (27b)$$

$$\omega_\mu = W(r) \delta_{\mu 0}. \quad (27c)$$

For the scalar meson σ and ϕ , we parameterize them as

$$\sigma = f_\pi (1 + \bar{\sigma}(r)), \quad (28a)$$

$$\phi = \phi_{\text{vac}} (1 + \bar{\phi}(r)), \quad (28b)$$

with $\bar{\sigma}(r)$ and $\bar{\phi}(r)$ being dimensionless functions. Substituting Eqs. (27) and (28) to the Lagrangian (12), one

can obtain the soliton mass and the equations of motion of the profile functions $F(r)$, $G(r)$, $W(r)$, $\bar{\sigma}(r)$ and $\bar{\phi}(r)$. The detailed expressions are given in Appendix B. For the solutions with baryon number $B = 1$, the wave functions of $F(r)$, $G(r)$ and $W(r)$ satisfy the boundary conditions

$$\begin{aligned} F(0) &= \pi, & F(\infty) &= 0, \\ G(0) &= -2, & G(\infty) &= 0, \\ W'(0) &= 0, & W(\infty) &= 0. \end{aligned} \quad (29)$$

The boundary conditions for the profile functions of the scalar mesons are determined in the following way. By considering that at $r \rightarrow \infty$ the VEVs of the scalar meson fields should be reproduced, so that both $\bar{\sigma}(r)$ and $\bar{\phi}(r)$ must vanish, i.e.,

$$\bar{\sigma}(\infty) = 0, \quad \bar{\phi}(\infty) = 0. \quad (30)$$

The second order derivative $\bar{\sigma}''$ and $\bar{\phi}''$ should not diverge at $r \rightarrow 0$. Then, the finiteness of the right hand sides of Eqs. (B6) and (B7) implies that the first derivatives of $\bar{\sigma}(r)$ and $\bar{\phi}(r)$ must vanish:

$$\bar{\sigma}'(0) = 0, \quad \bar{\phi}'(0) = 0. \quad (31)$$

The baryon number current of the present system can be obtained by introducing the corresponding external gauge field \mathcal{V}_μ of the $U(1)$ baryon number, and making a functional derivative with respect to \mathcal{V}_μ with the total action including the anomaly terms with Wess-Zumino action. We finally obtain the expression of the baryon number density B_0 as

$$\begin{aligned} B_0 = & -\frac{2}{3gr^2} \{ f_\pi^2 g^2 r^2 a_{\text{hls}} W [s_0 \bar{\sigma}^2 + 2s_0 \bar{\sigma} + 1] \\ & + F' [\alpha_2 - 2G(-\alpha_2 + \alpha_3 + \alpha_2 \cos F) + \alpha_2 \cos^2 F - 2\alpha_2 \cos F + (\alpha_2 - \alpha_3) G^2] \\ & - 2\alpha_3 \sin F G' + \alpha_1 \sin^2 F F' \} - \frac{\sin^2 F}{2\pi^2 r^2} F', \end{aligned} \quad (32)$$

where α_1 , α_2 and α_3 relate to c_1 , c_2 and c_3 through Eq. (B2). With the help of EoM for W in Eq. (B5), the baryon number density is simplified as

$$B_0 = \frac{1}{r^2} \frac{d}{dr} \left(\frac{4\alpha_3 \sin F (\cos F - G - 1)}{3g} - \frac{2r^2 W'}{3g} + \frac{\sin(2F)}{8\pi^2} - \frac{F}{4\pi^2} \right), \quad (33)$$

which agrees with the one obtained in Ref. [15]. It should be noted that, combining Eq. (33) with Eq. (29), one can show that the baryon charge is correctly normalized as $\int_0^\infty dr^3 B_0(r) = 1$.

In the present analyse, we take $c_1 + c_2 = 0$, $c_1 - c_2 = 3/4$ and $c_3 = 0$, therefore Eq. (32) is reduced to

$$B_0 = -\frac{2}{3gr^2} f_\pi^2 g^2 r^2 a_{\text{hls}} W [s_0 \bar{\sigma}^2 + 2s_0 \bar{\sigma} + 1]. \quad (34)$$

In our numerical calculation, in addition to the soliton mass, we also consider baryon number radius $\langle r^2 \rangle_B^{1/2}$ and

the mean square charge radius $\langle r^2 \rangle_E^{1/2}$ with the following definitions

$$\langle r^2 \rangle_B^{1/2} = \sqrt{\int_0^\infty d^3 r r^2 B_0(r)},$$

$$\langle r^2 \rangle_E^{1/2} = \sqrt{\frac{1}{M_{\text{sol}}} \int_0^\infty dr^3 r^2 M_{\text{sol}}(r)}, \quad (35)$$

where M_{sol} is the soliton mass and $M_{\text{sol}}(r)$ is the corresponding density given in Eq. (B1).

B. Effects of scalar mesons

Now we are in the position to show the effects of scalar mesons on skyrmion properties.

First, we consider the case $A = 0$ in which the four-quark state ϕ decouples from other mesons. The Lagrangian is reduced to

$$\mathcal{L} = \frac{1}{2} \partial_\mu \sigma \partial^\mu \sigma + \sigma^2 \text{Tr}(\alpha_{\perp\mu} \alpha_{\perp}^\mu) - (V_\sigma - \bar{V}_\sigma) - (V_{\text{SB}} - \bar{V}_{\text{SB}}) + \mathcal{L}_V, \quad (36)$$

with $V_\sigma = \frac{1}{8} \lambda \sigma^4 - \frac{1}{2} m_2^2 \sigma^2$. The parameters λ and m_2^2 are related to the masses of σ and π through

$$\begin{aligned} m_\sigma^2 &= -m_2^2 + \frac{3}{2} \lambda f_\pi^2, \\ m_\pi^2 &= -m_2^2 + \frac{1}{2} \lambda f_\pi^2. \end{aligned} \quad (37)$$

Here we take the empirical values of m_π as an input, and regard m_σ as a parameter of the model. In addition, s_0 in \mathcal{L}_V is a parameter not fixed. In the following, we study the effect of these two parameters in the skyrmion properties.

a. The effect of m_σ on the skyrmion properties. For this purpose, we take $s_0 = 0$. In this case, the \mathcal{L}_V part of the Lagrangian reduces to the standard form in the HLS [13].

We show the m_σ dependence of soliton mass m_{sol} , charge radii $\sqrt{\langle r^2 \rangle_B}$ and $\sqrt{\langle r^2 \rangle_E}$ in Fig. 1 and the profile functions in Fig. 2. From Fig. 1 we find that, with the increase of m_σ , the soliton mass m_{sol} increases. This tendency can be understood from the profile function of $\bar{\sigma}$ in Fig. 2: When the sigma meson becomes heavier, the magnitude of $\bar{\sigma}$ becomes smaller. Since $\bar{\sigma} < 0$, the magnitude of $\sigma = f_\pi(1 + \bar{\sigma})$ becomes larger and, consequently, the contribution from $\sigma^2 \text{Tr}(\alpha_{\perp\mu} \alpha_{\perp}^\mu)$ to the skyrmion mass becomes larger. Physically, for a heavier σ , the attractive force provided by the σ is smaller, and as a result, the soliton mass becomes larger.

In addition, Fig. 1 tells us that when m_σ becomes larger, the charge radii $\sqrt{\langle r^2 \rangle_E}$ and $\sqrt{\langle r^2 \rangle_B}$ become smaller. This result can be understood from the profile function plotted in Fig. 2: The larger m_σ is, the narrower profile for $\bar{\sigma}$ becomes. Generally, σ meson supplies the attractive force while ω meson supplies repulsive force. A narrower σ needs a narrower ω to make the balance of attractive force and repulsive force. The shape for σ and ω dominate the shape for energy distribution. Then, the narrower σ and ω make charge radius for energy $\sqrt{\langle r^2 \rangle_E}$ smaller. As for the charge radius of the baryon number density, from the baryon number density in Eq. (34)

with $s_0 = 0$, one can easily see that the narrower W gives smaller radius $\sqrt{\langle r^2 \rangle_B}$. To summarize, the effective range of the attractive force by the σ is smaller for larger m_σ , which makes the soliton size smaller.

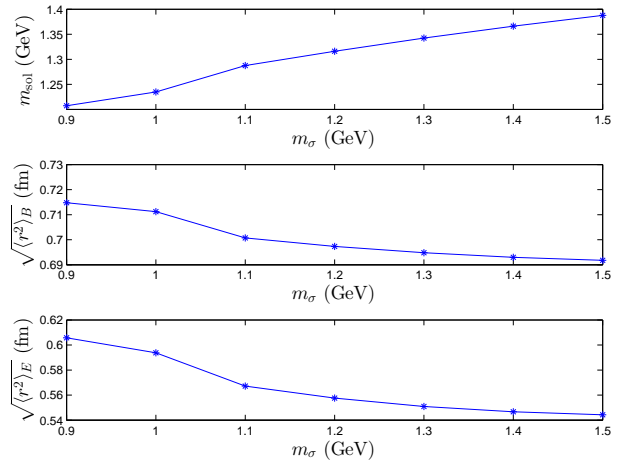


FIG. 1: m_σ dependence of the soliton mass and radii with $A = s_0 = 0$.

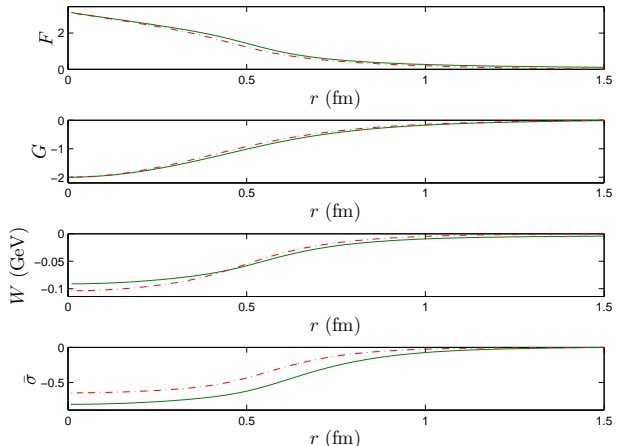


FIG. 2: m_σ dependence of the profile functions with $A = s_0 = 0$. Green curves correspond to $m_\sigma = 1$ GeV and red dotted curves to $m_\sigma = 1.4$ GeV.

b. The effect of s_0 on skyrmion properties. This study can tell us the effect of the two-quark condensate on the skyrmion properties through its effect on the vector meson mass. For this purpose, we take the typical scalar meson mass $m_\sigma = 1.37$. Our numerical results are plotted in Fig. 3.

From Fig. 3, we see that, the bigger s_0 is, the larger m_{sol} and $\sqrt{\langle r^2 \rangle_B}$ become. From the equations of motion for vector mesons in Eq. (B5), one can see that $a_{\text{hls}} g_\omega^2 (f_\pi^2 (1 - s_0) + s_0 \sigma^2(r))$ plays a role of an effective mass of vector mesons inside the soliton. Since $\sigma(r) < f_\pi$ as we stated above, the effective mass is smaller than the meson mass $m_\omega = \sqrt{a_{\text{hls}} g_\omega f_\pi}$ in the vacuum. Then, the

effective strength of repulsive force mediated by the ω meson is stronger for a larger s_0 , which makes the soliton mass bigger. The effective range of repulsive force is longer for a larger s_0 . Since the baryon number current is proportional to the effect of ω meson as can be seen in Eq. (34), the baryon number charge radius $\sqrt{\langle r^2 \rangle_B}$ becomes larger for a larger s_0 .

The situation for charge radius of energy $\sqrt{\langle r^2 \rangle_E}$ is quite complicated. In the present analysis, the numerical error is about 1-3%, so that the third graph in Fig. 4 implies that $\sqrt{\langle r^2 \rangle_E}$ is rather stable against the change of s_0 . This implies that the contribution from ω works in an opposite direction to the one from σ , and that they cancel with each other.

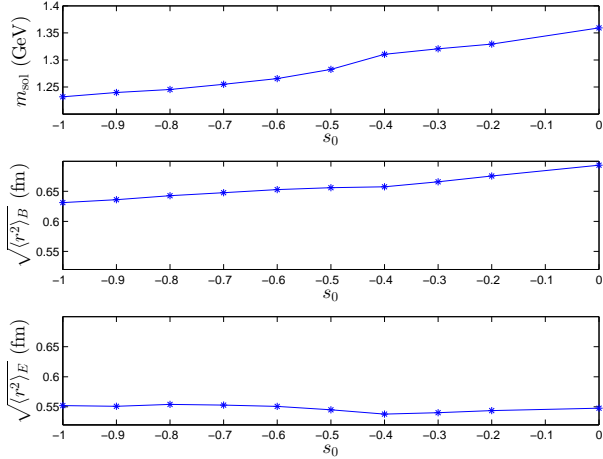


FIG. 3: s_0 dependence of the skyrmion mass and radii for $m_\sigma = 1.37$ GeV.

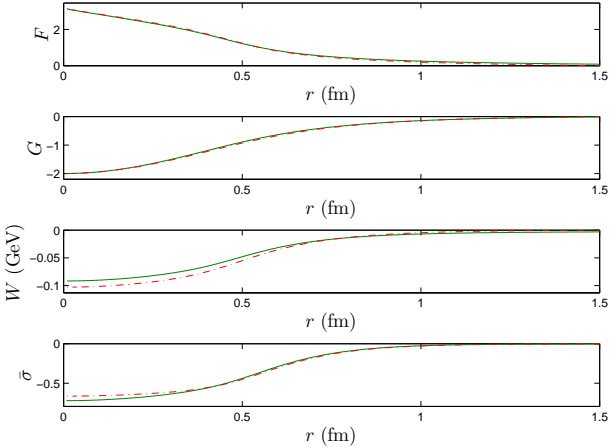


FIG. 4: The profile functions with $s_0 = -0.5$ (green line) and $s_0 = 0$ (red dotted line).

Next, we study the effect of mixing between the two scalar mesons on the skyrmion properties by setting $A \neq 0$. In our calculation, we take two fixed values of s_0 , $s_0 =$

0 and $s_0 = -0.5$, to see the dependence of the mass and the radii of the skyrmion on the mixing angle θ defined in Eq. (18). Our results are shown in Figs. 5 and 6. We

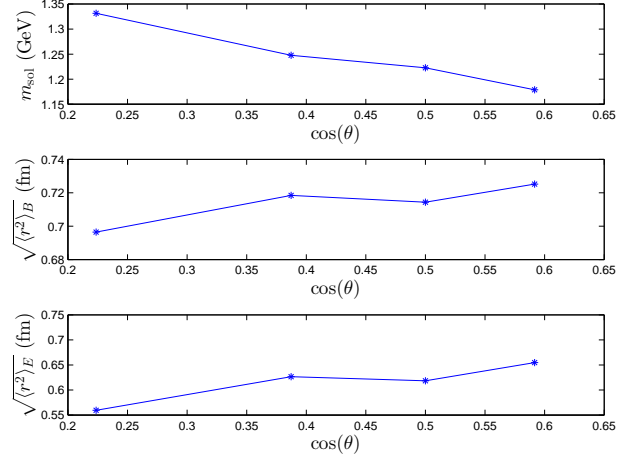


FIG. 5: Dependence on the mixing angle between two scalar mesons for $s_0 = 0$.

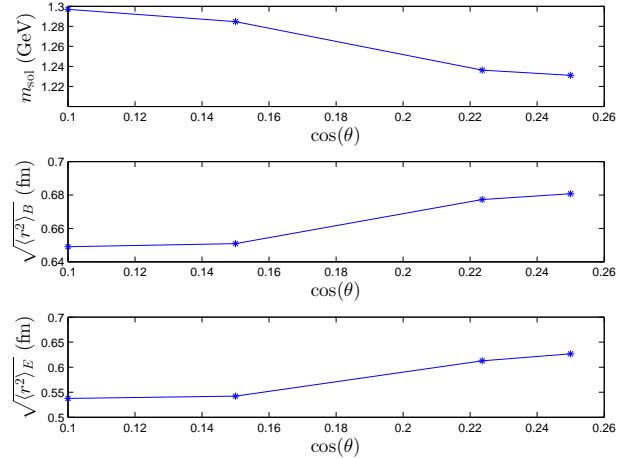


FIG. 6: Dependence on the mixing angle between two scalar mesons for $s_0 = -0.5$.

should note that we cannot find any stable solutions in the region of $\cos\theta > 0.6$ for $s_0 = 0$ and $\cos\theta > 0.25$ for $s_0 = -0.5$. In other words, the maximal value of $\cos\theta$ is smaller for smaller s_0 . This could be understood as follows: The definition of the mixing angle in Eq. (18) implies that, for a larger $\cos\theta$, the f_{500} includes more two-quark component $\tilde{\sigma}$, and the attractive force becomes stronger, and the soliton collapses at a certain value of $\cos\theta$. On the other hand, the decrease of s_0 means the repulsive force mediated by the ω becomes weaker, as we stated above. Since the soliton is stabilized by the balance between the attractive force and the repulsive force, the maximal $\cos\theta$ becomes smaller for a smaller

s_0 .

It should be noted that the decreasing and increasing tendencies in Figs. 5 and 6 are the same and they are actually consistent with the ones in Fig. 1. As we stated just above, increasing of $\cos\theta$ leads to the increasing of the magnitude of the two-quark component included in f_{500} . Then, the larger $\cos\theta$ in Figs. 5 and 6 correspond to a smaller mass in Fig. 1.

IV. CONCLUSIONS AND DISCUSSIONS

In this work, we first study the effects of scalar mesons on the skyrmion properties. We find that, when the mixing between the two-quark and four-quark states are switched off, the lighter two-quark scalar meson is, the smaller soliton mass becomes. The baryon number charge radius $\sqrt{\langle r^2 \rangle_B}$ and the mean square charge radius $\sqrt{\langle r^2 \rangle_E}$ become wider. We next study the skyrmion properties affected by the σ coupling to the vector mesons. It is found that the larger coupling becomes, the heavier the mass is and the larger the charge radii are. We finally explore the skyrmion properties by considering the mixing structure of the scalar mesons. We show that, with the increase of two-quark component in the light scalar meson, the soliton mass drops while $\sqrt{\langle r^2 \rangle_B}$ and $\sqrt{\langle r^2 \rangle_E}$ become larger.

Our numerical results show that, even though we include both the two-quark and four-quark scalar mesons in the model, the soliton spectrum is still about 300 MeV

larger than the empirical value of the classical soliton mass to reproduce the experimental value of the nucleon mass. So that, to establish a Skyrme type model that can reproduce the baryon mass, the present model should be extended. Several possible extensions are, for example, to include the effect of the dilaton as the Nambu-Goldstone boson associated with the scale symmetry breaking of QCD, to include the $\mathcal{O}(p^4)$ terms of HLS which account for the π - ρ interaction and to include all the homogeneous Wess-Zumino terms of HLS which include more π - ρ and π - ρ - ω terms. We leave such discussions in the future project. In addition, even though the present model cannot simulate the reality, it is still deserve to apply it to the dense system to study the effect of the scalar mesons on the phase structure of the nuclear matter. We will report this progress elsewhere.

ACKNOWLEDGMENTS

M. H. was supported in part by the JSPS Grant-in-Aid for Scientific Research (S) No. 22224003 and (c) No. 24540266. And the work of Y.-L. M. was supported in part by National Science Foundation of China (NSFC) under Grant No. 11475071 and the Seeds Funding of Jilin University.

Appendix A: The mixing matrix

The masses of f_{500} and f_{1370} are

$$m_{f_{500}}^2 = \frac{1}{2} \left(-\sqrt{2f_\pi^2 (4A^2 - \lambda m_4^2 + \lambda m_\pi^2) + f_\pi^4 \lambda^2 + (m_4^2 - m_\pi^2)^2} + f_\pi^2 \lambda + m_4^2 + m_\pi^2 \right), \quad (\text{A1})$$

$$m_{f_{1370}}^2 = \frac{1}{2} \left(\sqrt{2f_\pi^2 (4A^2 - \lambda m_4^2 + \lambda m_\pi^2) + f_\pi^4 \lambda^2 + (m_4^2 - m_\pi^2)^2} + f_\pi^2 \lambda + m_4^2 + m_\pi^2 \right). \quad (\text{A2})$$

The mixing angle θ can be obtained as

$$\theta = \arctan \sqrt{\frac{m_{f_{1370}}^2 - m_4^2}{m_4^2 - m_{f_{500}}^2}} = \arccos \sqrt{\frac{m_4^2 - m_{f_{500}}^2}{m_{f_{1370}}^2 - m_{f_{500}}^2}}. \quad (\text{A3})$$

From Eqs. (15), (16), (A1) and (A2), one gets

$$A^2 = \frac{(m_{f_{1370}}^2 - m_4^2)(m_4^2 - m_{f_{500}}^2)}{2f_\pi^2},$$

$$\lambda = \frac{m_{f_{500}}^2 + m_{f_{1370}}^2 - m_4^2 - m_\pi^2}{f_\pi^2},$$

$$\phi_{\text{vac}} = -\frac{Af_\pi^2}{\sqrt{2}m_4^2},$$

$$m_2^2 = \frac{1}{2} \left(\frac{m_{f_{500}}^2 m_{f_{1370}}^2}{m_4^2} - 3m_\pi^2 \right), \quad (\text{A4})$$

with $m_{f_{500}}^2 < m_4^2 < m_{f_{1370}}^2$.

Appendix B: Soliton mass and the equations of motion for the profile functions $F(r), G(r), W(r), \bar{\sigma}(r)$ and $\bar{\phi}(r)$

By using the profile functions defined in Eqs. (27) and (28) and the effective Lagrangian (12), one express soliton mass as

$$\begin{aligned}
M_{\text{sol}} &= 4\pi \int_0^\infty dr r^2 M_{\text{sol}}(r) \\
&= -4\pi \int_0^\infty dr \left\{ \frac{1}{8} r^2 \left\{ 4f_\pi^2 g^2 s_0 a_{\text{hls}} W^2 \bar{\sigma} (\bar{\sigma} + 2) - 4f_\pi^2 (\bar{\sigma} + 1)^2 F'^2 \right. \right. \\
&\quad + f_\pi^2 \left[\frac{2(m_4^2 - m_{f_{500}}^2)(m_{f_{1370}}^2 - m_4^2)(\bar{\sigma} + 1)^2 (\bar{\phi} + 1)}{m_4^2} - (m_{f_{500}}^2 + m_{f_{1370}}^2 - m_4^2 - m_\pi^2)(\bar{\sigma} + 1)^4 \right. \\
&\quad + \frac{2(m_{f_{500}}^2 m_{f_{1370}}^2 - 3m_4^2 m_\pi^2)(\bar{\sigma} + 1)^2}{m_4^2} + \frac{(m_4^2 - m_{f_{500}}^2)(m_4^2 - m_{f_{1370}}^2)(\bar{\phi} + 1)^2}{m_4^2} + 8m_\pi^2 (\bar{\sigma} + 1) \cos(F) \Big] \\
&\quad + \left. \left. \frac{f_\pi^2 (m_4^2 - m_{f_{500}}^2)(m_4^2 - m_{f_{1370}}^2) \bar{\phi}'^2}{m_4^4} - 4f_\pi^2 \bar{\sigma}'^2 + 4f_\pi^2 g^2 a_{\text{hls}} W^2 - \frac{f_\pi^2 (m_{f_{500}}^2 m_{f_{1370}}^2 + 3m_4^2 m_\pi^2)}{m_4^2} + 4W'^2 \right\} \right. \\
&\quad - \frac{1}{2g^2} \left\{ 8f_\pi^2 g^2 a_{\text{hls}} G \sin^2 \left(\frac{F}{2} \right) (s_0 \bar{\sigma}^2 + 2s_0 \bar{\sigma} + 1) - 4f_\pi^2 g^2 \bar{\sigma}^2 \sin^2 \left(\frac{F}{2} \right) ((s_0 a_{\text{hls}} - 1) \cos(F) - s_0 a_{\text{hls}} - 1) \right. \\
&\quad - 8f_\pi^2 g^2 \bar{\sigma} \sin^2 \left(\frac{F}{2} \right) ((s_0 a_{\text{hls}} - 1) \cos(F) - s_0 a_{\text{hls}} - 1) + 2f_\pi^2 g^2 a_{\text{hls}} G^2 (s_0 \bar{\sigma}^2 + 2s_0 \bar{\sigma} + 1) \\
&\quad + 8f_\pi^2 g^2 a_{\text{hls}} \sin^4 \left(\frac{F}{2} \right) - f_\pi^2 g^2 \cos(2F) + f_\pi^2 g^2 + 2G'^2 \Big\} \\
&\quad - \alpha_3 (2G(WF' - \sin(F)W') + G^2 WF' + 2\sin(F)((\cos(F) - 1)W' + WG')) \\
&\quad \left. + \alpha_2 WF'(-\cos(F) + G + 1)^2 + \alpha_1 WF' \sin^2(F) - \frac{G^2(G + 2)^2}{2g^2 r^2} \right\}. \tag{B1}
\end{aligned}$$

With

$$\alpha_1 = \frac{3gN_c}{16\pi^2}(c_1 - c_2), \alpha_2 = \frac{gN_c}{16\pi^2}(c_1 + c_2), \alpha_3 = \frac{gN_c}{16\pi^2}c_3. \tag{B2}$$

The equations of motion for $F(r), G(r), W(r), \bar{\sigma}(r)$ and $\bar{\phi}(r)$ are expressed as

$$\begin{aligned}
F'' &= \frac{1}{f_\pi^2 r^2 (1 + \bar{\sigma})^2} \\
&\quad \times \left\{ 2G (f_\pi^2 s_0 a_{\text{hls}} \bar{\sigma}^2 \sin F + 2f_\pi^2 s_0 a_{\text{hls}} \bar{\sigma} \sin F + f_\pi^2 a_{\text{hls}} \sin F \right. \\
&\quad - \alpha_2 \cos F W' - \alpha_3 \cos F W' + \alpha_2 W G' - \alpha_3 W G' + \alpha_2 W' - \alpha_3 W') \\
&\quad - f_\pi^2 \bar{\sigma} \sin F (4s_0 a_{\text{hls}} \cos F - 4s_0 a_{\text{hls}} - 4 \cos F - r^2 m_\pi^2) - 2f_\pi^2 \bar{\sigma}^2 \sin F (s_0 a_{\text{hls}} \cos F - s_0 a_{\text{hls}} - \cos F) \\
&\quad - 2f_\pi^2 r^2 F' \bar{\sigma}' - 2f_\pi^2 r \bar{\sigma}^2 F' - 2f_\pi^2 r \bar{\sigma} F' (r \bar{\sigma}' + 2) + 2f_\pi^2 a_{\text{hls}} \sin F - f_\pi^2 a_{\text{hls}} \sin(2F) \\
&\quad - 2f_\pi^2 r F' + f_\pi^2 m_\pi^2 r^2 \sin F + f_\pi^2 \sin(2F) - 2\alpha_2 W \cos F G' + 2\alpha_3 W \cos F G' \\
&\quad - \frac{1}{2} \alpha_1 \cos(2F) W' - 2\alpha_2 \cos F W' + \frac{1}{2} \alpha_2 \cos(2F) W' - 2\alpha_3 \cos F W' + 2\alpha_3 \cos(2F) W' + 2\alpha_2 W G' \\
&\quad \left. - 2\alpha_3 W G' + (\alpha_2 - \alpha_3) G^2 W' + \frac{1}{2} \alpha_1 W' + \frac{3}{2} \alpha_2 W' \right\}, \tag{B3}
\end{aligned}$$

$$\begin{aligned}
G'' &= -f_\pi^2 g^2 a_{\text{hls}} (s_0 \bar{\sigma}^2 + 2s_0 \bar{\sigma} + 1) (\cos F - G - 1) - \alpha_3 g^2 (WF'(\cos F - G - 1) + 2\sin F W') \\
&\quad + \alpha_2 g^2 WF'(\cos F - G - 1) + \frac{G(G^2 + 3G + 2)}{r^2}, \tag{B4}
\end{aligned}$$

$$\begin{aligned}
W'' &= f_\pi^2 g^2 a_{\text{hls}} W (s_0 \bar{\sigma}^2 + 2s_0 \bar{\sigma} + 1) - \frac{2W'}{r} \\
&\quad + \frac{1}{r^2} \left\{ -\alpha_3 (F' (2G(\cos F + 1) + 2(\cos F - \cos(2F))) + G^2) + 4\sin F G' \right. \\
&\quad \left. + \alpha_2 F'(-\cos F + G + 1)^2 + 2\alpha_1 F' \sin^2 \left(\frac{F}{2} \right) (\cos F + 1) \right\}, \tag{B5}
\end{aligned}$$

$$\begin{aligned}
\bar{\sigma}'' = \frac{1}{2m_4^2} & \left\{ m_4^2 (2\bar{\sigma} (-g^2 s_0 a_{\text{hls}} W^2 + m_{f_{500}}^2 + m_{f_{1370}}^2 + F'^2 - m_4^2) + (m_{f_{500}}^2 + m_{f_{1370}}^2 - m_4^2 - m_\pi^2) \bar{\sigma}^3 \right. \\
& + 3 (m_{f_{500}}^2 + m_{f_{1370}}^2 - m_4^2 - m_\pi^2) \bar{\sigma}^2 + 2 [-g^2 s_0 a_{\text{hls}} W^2 + F'^2 - m_\pi^2 (\cos F - 1)] \\
& \left. - (m_4^2 - m_{f_{500}}^2) (m_{f_{1370}}^2 - m_4^2) (\bar{\sigma} + 1) \bar{\phi} \right\} \\
& - \frac{(\bar{\sigma} + 1) (-8s_0 a_{\text{hls}} G \sin^2(\frac{F}{2}) - 8s_0 a_{\text{hls}} \sin^4(\frac{F}{2}) - 2s_0 a_{\text{hls}} G^2 + \cos(2F) - 1)}{r^2} - \frac{2\bar{\sigma}'}{r}, \tag{B6}
\end{aligned}$$

$$\bar{\phi}'' = m_4^2 (\bar{\phi} - \bar{\sigma} (\bar{\sigma} + 2)) - \frac{2\bar{\phi}'}{r}. \tag{B7}$$

-
- [1] T. H. R. Skyrme, Nucl. Phys. **31**, 556 (1962).
- [2] For a comprehensive collection of the progress, see G.E. Brown and M. Rho, ed. *The multifaceted skyrmion* (World Scientific, Singapore 2010).
- [3] For a review of early progress in this aspect, see, e.g., I. Zahed and G. E. Brown, Phys. Rept. **142**, 1 (1986).
- [4] For a review, see B. -Y. Park and V. Vento, “Skyrmion approach to finite density and temperature,” arXiv:0906.3263 [hep-ph], in *The Multifaceted Skyrmions* (World Scientific, Singapore, 2010) ed. G. E. Brown and M. Rho.
- [5] P. Sutcliffe, JHEP **1104**, 045 (2011).
- [6] Y. L. Ma, Y. Oh, G. S. Yang, M. Harada, H. K. Lee, B. Y. Park and M. Rho, Phys. Rev. D **86**, 074025 (2012) [arXiv:1206.5460 [hep-ph]].
- [7] Y. L. Ma, G. S. Yang, Y. Oh and M. Harada, Phys. Rev. D **87**, no. 3, 034023 (2013) [arXiv:1209.3554 [hep-ph]].
- [8] B. Y. Park, M. Rho and V. Vento, Nucl. Phys. A **736**, 129 (2004) [hep-ph/0310087].
- [9] B. Y. Park, M. Rho and V. Vento, Nucl. Phys. A **807**, 28 (2008) [arXiv:0801.1374 [hep-ph]].
- [10] Y. L. Ma, M. Harada, H. K. Lee, Y. Oh, B. Y. Park and M. Rho, Phys. Rev. D **90**, no. 3, 034015 (2014) [arXiv:1308.6476 [hep-ph]].
- [11] A. H. Fariborz, R. Jora and J. Schechter, Phys. Rev. D **79**, 074014 (2009) [arXiv:0902.2825 [hep-ph]].
- [12] M. Bando, T. Kugo and K. Yamawaki, Phys. Rept. **164**, 217 (1988).
- [13] M. Harada and K. Yamawaki, Phys. Rept. **381**, 1 (2003) [hep-ph/0302103].
- [14] U. G. Meissner, N. Kaiser and W. Weise, Nucl. Phys. A **466**, 685 (1987).
- [15] U. G. Meissner, N. Kaiser, H. Weigel and J. Schechter, Phys. Rev. D **39**, 1956 (1989) [Erratum-ibid. D **40**, 262 (1989)].